ELECTROMECHANICAL STUDY OF MICROMACHINED ELECTROSTATIC PARALLEL-PLATE ACTUATORS

J. De Coster, F. Henrotte, K. Hameyer, R. Puers
Katholieke Universiteit Leuven, Dept. ESAT, Kasteelpark Arenberg 10
B-3001 Heverlee-Leuven, Belgium
E-mail: **jeroen.decoster@esat.kuleuven.ac.be**

Abstract **—** *Electrostatic actuators are commonplace in many kinds of microelectromechanical devices (MEMS). For such applications as RF tunable capacitors, the device performance depends critically on the exact deformation of the suspended membrane. FEM models are very well suited to provide insight in this deformation [1], and the development of an efficient electromechanical model is the subject of this paper. The model size is reduced by partially decoupling the mechanical and electrical design, and further advantage is taken of this approach in order to reduce the number of iterations required per voltage step.*

Introduction

MEMS devices are fabricated using micro fabrication techniques and equipment similar to those used in traditional IC-making processes. A sequence of layer deposition, patterning and underetching steps leads to a parallel-plate actuator like the one shown in fig. 1. The parallel-plate actuator consists of a fixed bottom electrode, on top of which a thin dielectric layer is deposited. The top electrode can move in the vertical direction and is suspended with mechanically compliant suspension beams (represented schematically in fig. 1a and c). In order to facilitate underetching, access holes are patterned in the top electrode. The geometry of the FEM model presented in this paper is parameterized in order to easily accommodate layer thicknesses and access hole dimensions for any given process flow.

When a DC bias voltage is applied across the top and bottom electrode-pair (as shown in fig. 1c), an attractive electrostatic force is generated which pulls the top electrode towards the substrate. As a consequence, the capacitance can be fine-tuned by regulating the applied bias voltage. Beyond a

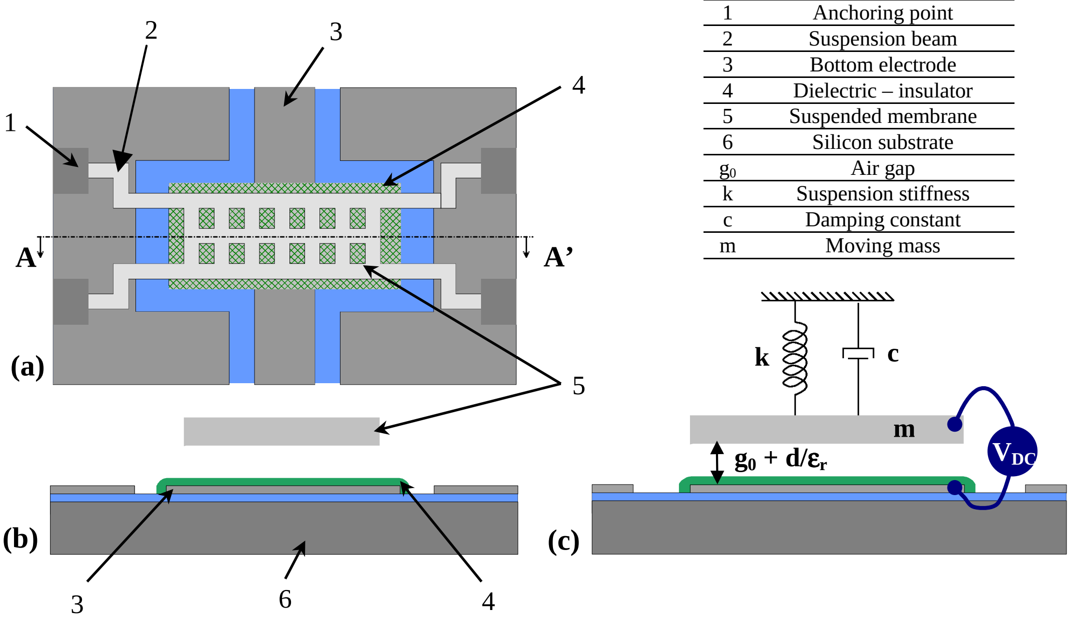

1	Anchoring point
2	Suspension beam
3	Bottom electrode
4	Dielectric – insulator
5	Suspended membrane
6	Silicon substrate
g_0	Air gap
k	Suspension stiffness
c	Damping constant
m	Moving mass

Fig. 1. (a) Top view and (b) cross-section of a micromachined parallel-plate actuator. The mechanical properties are depicted in (c).

certain threshold value however, there is no equilibrium point anymore and the top electrode collapses onto the substrate. This phenomenon is called the ‘pull-in’ of the electrostatic actuator. The purpose of the electromechanical simulation dealt with in this paper, is to find the capacitance as a function of the applied bias voltage and to calculate the voltage threshold where pull-in occurs.

Decoupling the mechanical and electrical design

Two distinct parts can be identified in the mechanical domain of the parallel-plate actuator: the membrane and the suspension beams [2]. The former is intimately coupled to the electrical domain, since a deformation of the membrane directly affects the capacitance as well as the attractive electrostatic force. The deformation of the suspension beams on the other hand, has a negligible influence on the electrical quantities in the system since there is no overlap between the beams and the bottom electrode. The suspension beams can therefore be decoupled from the electrostatic problem and as such they can be represented by means of ideal springs. This yields the following flowchart for the electromechanical simulation of parallel-plate actuators:

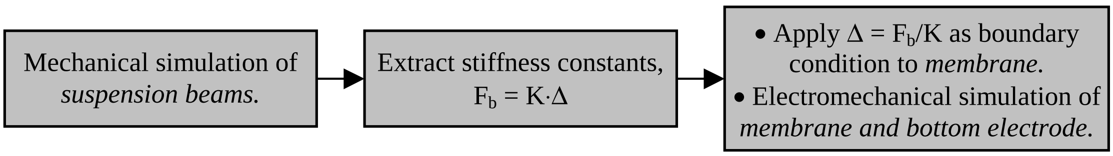

Figure 2. Flowchart of electromechanical simulation of parallel-plate actuator.

Put another way, the mechanical design of the suspension beams can be done independently from the membrane design. Moreover, leaving out the suspension beams reduces the size and the computation time of the electromechanical problem.

Test Problem

The approach illustrated in fig. 2 is applied to the simulation of an RF MEMS tunable capacitor. The left part of fig. 3 shows the layout of the MEMS device. The membrane measures $275\text{x}125\mu m^2$ and has a thickness of 5µm, the nominal zero-voltage air gap is 3µm thick and the dielectric on top of the bottom electrode has a thickness of 0.2µm and a relative premittivity of 7. The access holes for underetching have a pitch of 50µm and their width is 25µm.

The mechanical part of the parameterized model is depicted in the right hand side of fig. 3, and the electrical domain consists of the air volume surrounding it. The finite element mesh of

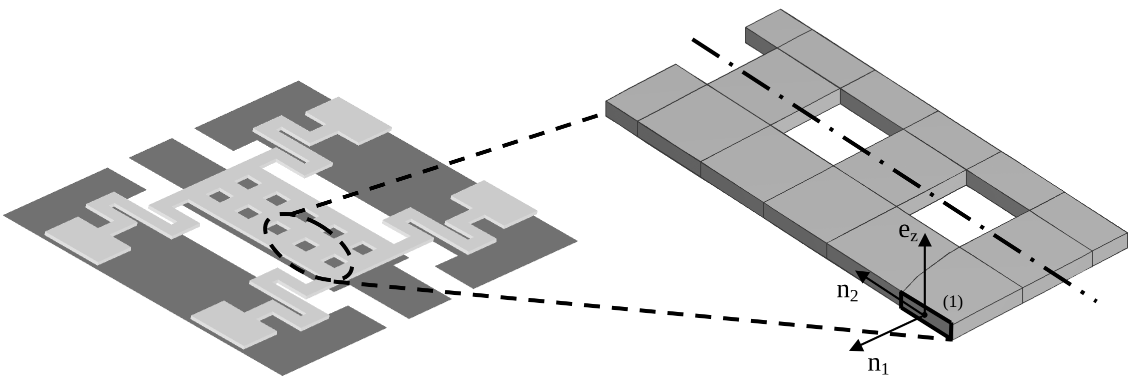

Fig. 3. Layout of an RF MEMS tunable capacitor and mechanical membrane model.

the electrical domain contains 3942 nodes and 15303 first-order tetrahedra. The linear static system is solved using an iterative solver available in the Femlab® finite element environment [3] and fig. 4 shows the computed electric potential along a slice indicated by the dotted line in fig. 3. The capacitance of the device is found in terms of the electrostatic energy of the entire domain:

$$C = 4 \cdot \frac{2W_e}{V_{DC}^2} \tag{1}$$

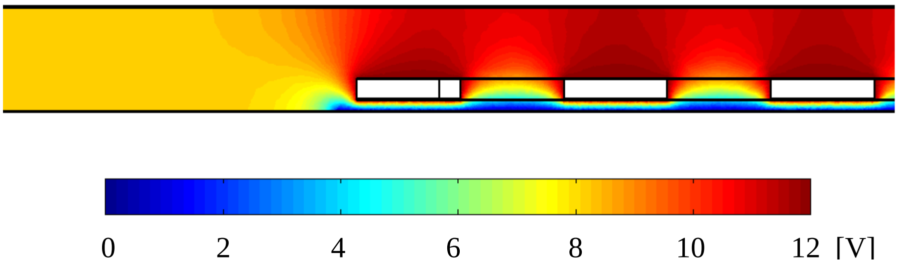

Figure 4. Electrostatic potential in the air volume surrounding the membrane.

The computed electric field is used to determine the force distribution applied to the mechanical problem. In a typical electrostatic actuator, the suspension beams represent 20% of the mechanical domain volume. As a consequence, the approach outlined in fig. 2 results in a reduction by 20%of the mechanical problem size. The finite element mesh in the test problem consists of 657 nodes and 2096 second-order elements. Symmetry boundary conditions are applied along the axes of symmetry and the attractive electrostatic force density that is applied to the underside of the membrane is found by calculating the zz-component of the Maxwell stress tensor at the surface of the membrane:

$$f_e = \frac{F_z}{A} = \varepsilon_0 E_z^2 - \frac{\varepsilon_0 |E|^2}{2} \tag{2}$$

where f_e is the electrostatic force density attracting the membrane, E is the electric field and z is the coordinate perpendicular to the membrane in its undeflected state.

The patch indicated as (1) in fig. 3, is the patch that would normally be coupled with the suspension beam. Since the beam is represented by its stiffness constants, a displacement boundary condition is used for this patch. The value of the vertical displacement is found by dividing the resultant electrostatic force (integration of (2)) by the stiffness constant of the suspension:

$$\Delta = \frac{F}{K} = \frac{1}{K} \int_S f_e \, dS \tag{3}$$

where S is the membrane surface and K is the transverse loading stiffness constant of the suspension. Similarly, if the stiffness constant for rotation around n_2 is denoted by K_B, the tilting angles α (rotation about n_2) and θ (rotation about n_1) of the patch can be found as:

$$\alpha = \frac{M_b}{K_B} = \frac{1}{K_B} \int_S ((\vec{x} - \vec{x}_1) \times f_e \vec{e}_z) \cdot \vec{n}_2 \, dS \qquad \theta = \frac{M_t}{K_T} = \frac{1}{K_T} \int_S ((\vec{x} - \vec{x}_1) \times f_e \vec{e}_z) \cdot \vec{n}_1 \, dS \tag{4}$$

where x is the space coordinate, x_1 is the coordinate of the midpoint of the patch indicated in fig. 3, n_1 is its normal, K_T is the torsional stiffness constant and n_2 is parallel with the patch and with the membrane surface.

Results

Numerical computations with varying bias voltages yield the C-V characteristic of the tunable capacitor. From fig. 5a, it can be seen that pull-in occurs at 25V: the computation converges for an applied bias voltage of 24.5V, whereas the membrane displacement exceeds the air gap thickness when 25V is applied. Measurements on prototypes [4] have shown an average pull-in voltage of 27.5V. Another important quantity for electrostatic actuators is the reversible tuning range (TR), which is defined as the relative capacitance change before pull-in occurs:

$$TR = \frac{C_{V_{PI}} - C_0}{C_0} \tag{5}$$

The electromechanical simulations show that the reversible tuning range for the test problem is 40%.

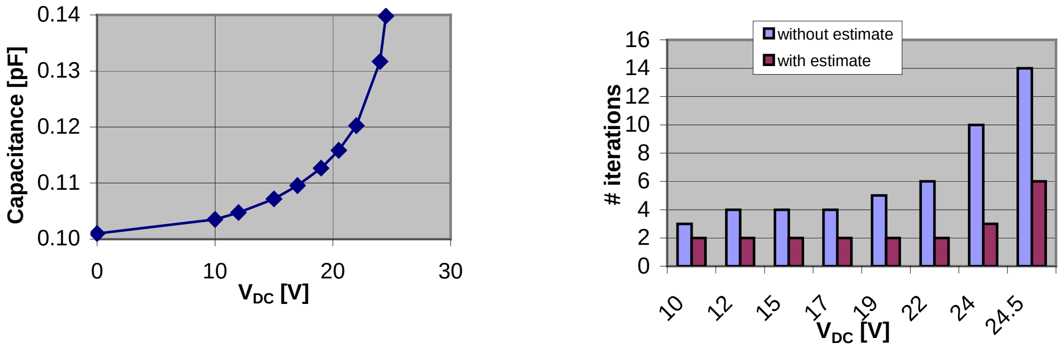

Figure 5. (a) Simulated capacitance versus bias voltage tuning characteristic and (b) number of iterations per voltage step, with and without analytical estimate.

Apart from reducing the computation time needed for a single electromechanical calculation, the approach outlined in fig. 2 has the additional advantage of allowing the finite element calculations to be combined with an analytical estimate of the membrane displacement. This allows for a reduction of the number of iterations per electromechanical solution. The estimate is obtained by iterative solution of the following equation for the displacement x:

$$Kx = \frac{V_{DC}^2 A \varepsilon_0}{2(g_0 + d/\varepsilon_r - x)^2} \tag{6}$$

where the symbols can be found in fig. 1. Fig. 5b shows a comparison of the number of iterations in the test problem with and without analytical estimate, to reach a relative displacement accuracy of $5{\cdot}10^{-3}$.

Conclusions

An electromechanical model has been presented that provides the MEMS designer with accurate values of the pull-in voltage and tuning ratio of electrostatic actuators. A partial decoupling of the mechanical and electrical problem definition allows for faster computation of the actuator's electrical behavior and the number of iterations per voltage step was reduced by combining the FEM calculations with analytical estimates. There is a difference of approximately 10% between the calculated and measured pull-in voltage, which is rather accurate considering the relatively large process-related non-ideality.

References

[1] J. R. Gilbert et al., 3D Coupled Electro-mechanics for MEMS: Applications of CoSolve EM, Proc. Conf. MEMS '95, pp. 122-127, 1995.

[2] S. V. Ivyr and T. Mukherjee, Numerical Spring Models for Behavioral simulation of MEMS inertial sensors, Proc. Conf. DTIP '00, pp. 55-62, 2000.

[3] http://www.euro.femlab.com/

[4] J. van Beek et al, High-Q integrated passives and micromechanical capacitors on silicon (invited. paper), *Proc. BCTM '03*, 2003.